

Deficient plastidic fatty acid synthesis triggers cell death by modulating mitochondrial reactive oxygen species

Jian Wu^{1,*}, Yuefeng Sun^{1,2,*}, Yannan Zhao¹, Jian Zhang¹, Lilan Luo¹, Meng Li¹, Jinlong Wang¹, Hong Yu¹, Guifu Liu¹, Liusha Yang¹, Guosheng Xiong¹, Jian-Min Zhou¹, Jianru Zuo¹, Yonghong Wang¹, Jiayang Li¹

¹State Key Laboratory of Plant Genomics and National Center for Plant Gene Research (Beijing), Institute of Genetics and Developmental Biology, Chinese Academy of Sciences, Beijing 100101, China

Programmed cell death (PCD) is of fundamental importance to development and defense in animals and plants. In plants, a well-recognized form of PCD is hypersensitive response (HR) triggered by pathogens, which involves the generation of reactive oxygen species (ROS) and other signaling molecules. While the mitochondrion is a master regulator of PCD in animals, the chloroplast is known to regulate PCD in plants. *Arabidopsis* Mosaic Death 1 (MOD1), an enoyl-acyl carrier protein (ACP) reductase essential for fatty acid biosynthesis in chloroplasts, negatively regulates PCD in *Arabidopsis*. Here we report that PCD in *mod1* results from accumulated ROS and can be suppressed by mutations in mitochondrial complex I components, and that the suppression is confirmed by pharmaceutical inhibition of the complex I-generated ROS. We further show that intact mitochondria are required for full HR and optimum disease resistance to the *Pseudomonas syringae* bacteria. These findings strongly indicate that the ROS generated in the electron transport chain in mitochondria plays a key role in triggering plant PCD and highlight an important role of the communication between chloroplast and mitochondrion in the control of PCD in plants.

Keywords: cell death; PPR protein; ETC; ROS; mitochondria; chloroplasts; *Arabidopsis thaliana*

Cell Research (2015) 25:621–633. doi:10.1038/cr.2015.46; published online 24 April 2015

Introduction

Programmed cell death (PCD) is a genetically regulated process of cell suicide, which is essential for both development and defense response in multicellular organisms [1]. In animals, mitochondria play a central role in initiating PCD by integrating diverse stress signals [2] and the intracellular homeostasis of reactive oxygen species (ROS) is crucial in regulating cell death and cell survival [3]. In plants, several compartments contribute to the formation of ROS, including the plasma membrane, peroxisomes, chloroplasts and mitochondria. ROS synthesized by the plasma membrane NADPH oxidases

has been considered to play a role in the hypersensitive response (HR), a type of PCD triggered by pathogens [4]. Chloroplasts are also considered to play an important role in HR since chloroplasts are the major ROS sources under excess of excitation energy conditions [5, 6]. However, a role of mitochondria remains obscure, so does the role of the ROS generated in the mitochondria during cell death in plants. In particular, it remains unclear whether ROS generated in the mitochondria is essential and sufficient to trigger PCD.

In mitochondria, ROS is inevitably produced during ATP synthesis. Several redox centers, mainly complexes I and III, of the mitochondrial electron transport chain (ETC) release electrons to molecular oxygen, serving as the primary source of superoxide formation [7]. Meanwhile, plants have adopted sophisticated mechanisms to remove excessive ROS to avoid the potential damage to cells [8]. Among the ROS scavenging enzymes, superoxide dismutases (SOD) dismutate superoxide anion (O_2^-) to hydrogen peroxide (H_2O_2), which is subsequently converted into H_2O by catalases or peroxidases [8].

Eukaryotic complex I (NADH:quinone oxidoreduc-

*These two authors contributed equally to this work.

Correspondence: Jiayang Li

Tel: +86-10-6480-6577; Fax: +86-10-6480-6595

E-mail: jyli@genetics.ac.cn

²Current address: Department of Pathology and Cell Biology, University of South Florida, Tampa, FL 33612, USA

Received 3 October 2014; revised 6 January 2015; accepted 27 February 2015; published online 24 April 2015

tase, EC 1.6.5.3) is a mitochondrial redox center assembled by the inner membrane-bound proteins, which catalyzes the transfer of two electrons from NADH to ubiquinone along with the translocation of four protons from the matrix compartment to the intermembrane space. This well-studied large complex contains at least 46 subunits in mammals [9, 10] and more than 49 subunits in plants, 17 of which are unique to plants [11]. Most plant complex I subunits are encoded by the nuclear genome, except for nine (named *NAD*) which are encoded by the mitochondrial genome [12]. While a few subunits have been partially characterized, the functions of most complex I subunits are still unknown [13]. Of those characterized mutants that carry lesions in subunits of complex I or nuclear-encoded regulators, all show dysfunction of complex I, with various defects in the ETC activity, cellular energy metabolism, ROS homeostasis and stress tolerance [14-23].

The fact that most of the mitochondrial proteins are encoded by the nuclear genome and a small number of proteins by the mitochondrial genome suggests a coordinated regulation of the mitochondrial proteome to maintain their functions. The genome-coordinating mechanisms need reciprocal communications, including anterograde (nucleus to organelle) and retrograde (organelle to nucleus) signals [24]. The anterograde control of organelle gene expression is primarily post-transcriptionally regulated by nuclear-encoded regulators. One of these regulators is pentatricopeptide repeat (PPR) proteins, which are characterized by the signature motif of a degenerate 35-amino-acid repeat often arranged in tandem arrays of up to 30 repeats [25, 26]. In animal and fungal genomes, the number of PPR genes is relatively small. However, in plants the size of this gene family is greatly expanded. There are 450 and 477 PPR proteins in *Arabidopsis* and rice, respectively [27, 28]. Plant PPR proteins are classified into P and PLS subfamilies. The PLS subfamily can be further divided into E, E+ and DYW groups based on their specific C-terminal motifs [27]. Most of the PPR proteins are predicted to target mitochondria or chloroplasts and to bind specific organellar RNAs for posttranscriptional processing, such as RNA editing, splicing, degradation and translation in mitochondria and chloroplasts [24, 26]. The functions of PPR proteins are highly diverse; they may participate in many aspects of plant development, such as embryogenesis and cytoplasmic male sterility.

Our previous studies have shown that the *Arabidopsis mosaic death 1 (mod1)* is a cell death mutant [29], which results from the deficiency in enoyl-acyl carrier protein (ACP) reductase, a subunit of the fatty acid synthase complex that catalyzes the *de novo* biosynthesis of fatty

acids in plastids. In this paper, we show that the ROS generated in mitochondrial ETC plays a crucial role in triggering the PCD in *mod1* originated from the deficiency of fatty acid biosynthesis in plastids.

Results

Accumulation of ROS in *mod1*

Our previous study showed that the fatty acid biosynthetic mutant *mod1* displays pleiotropic phenotypes characteristics of typical PCD features, including irregular cell sizes and shapes, disorganized cellular structures, DNA laddering and consequent cell death [29]. Oxidative burst leading to local ROS accumulation is usually regarded as a critical event associated with plant cell death [30, 31]. We therefore compared the accumulation of ROS (H_2O_2 and O_2^-) between *mod1* and wild-type plants by staining with 3,3'-diaminobenzidine (DAB) and nitroblue tetrazolium (NBT), respectively. As shown in Figure 1, both H_2O_2 and O_2^- are remarkably accumulated in *mod1* leaves, suggesting that the accumulation of ROS may play an important role in triggering cell death in *mod1*.

SOM3 protein is a subunit of the mitochondrial ETC complex I

To elucidate the molecular mechanism underlying cell death in *mod1* plants, we screened various suppressors

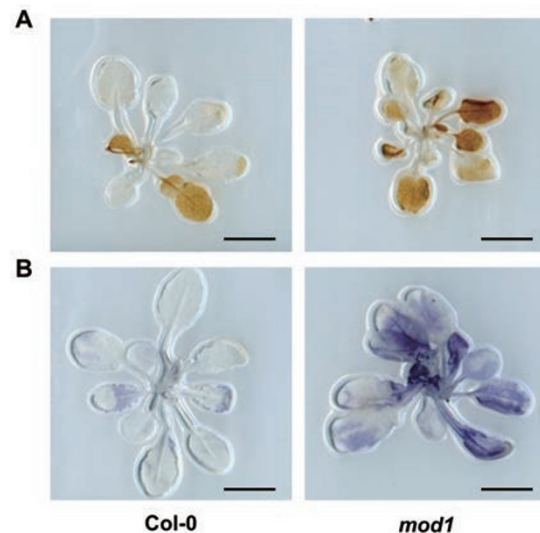


Figure 1 Comparison of ROS levels between wild-type and *mod1* plants. **(A)** Seedlings stained with 3,3'-diaminobenzidine (DAB), showing the H_2O_2 levels in wild-type (Col-0) and *mod1* plants. Scale bar, 1 cm. **(B)** Seedlings stained with nitroblue tetrazolium (NBT), showing O_2^- in Col-0 and *mod1* plants. Scale bar, 1 cm.

of *mod1* (*som*) through T-DNA insertion mutagenesis. Among them, a recessive mutant, *mod1 som3-1*, showed not only a similar morphological phenotype to the wild type (Figure 2A), but also an apparent reduction in cell death (Figure 2B) and in the accumulation of H₂O₂ (Figure 2C) and O₂⁻ (Figure 2D). Thus, *som3* is indeed a suppressor of *mod1*.

To clone *SOM3*, we amplified the inserted T-DNA and its flanking sequences through TAIL-PCR. A T-DNA insertion was found in the first intron of *AT1G47260* (Figure 2E), which disturbs the formation of the transcripts of *AT1G47260* (Figure 2F), consistent with the recessive inheritance of *som3*. To verify that suppression of the *mod1* phenotypes was a result of the null mutation of *AT1G47260*, we generated transgenic plants expressing a full-length cDNA of *AT1G47260* under the control of the Cauliflower Mosaic Virus 35S promoter (35S). The complemented plants restored the *mod1* phenotypes (Figure 2A-2D). Another allele, *salk_010194* (*som3-2*), which contains a T-DNA insertion in the third exon of *AT1G47260*, also suppressed the phenotypes of *mod1* (Figure 2A-2D). Therefore, *AT1G47260* is the corresponding *SOM3* gene, whose null mutation is responsible for the suppression of the *mod1* phenotypes.

To confirm the subcellular localization of *SOM3*, a 35S:*SOM3-GFP* transgene was stably expressed in *mod1 som3* plants and was capable of restoring the *mod1* phenotypes, demonstrating that the *SOM3-GFP* transgene is fully functional *in planta*. The GFP fluorescent signal was co-localized with the MitoTracker Red marker (Figure 2G), a dye which specifically stains mitochondria. These data clearly showed that the *SOM3* protein is specifically localized in mitochondria, which is consistent with the observations made in previous studies [15, 32, 33]. As expected, *MOD1*, a key enzyme of fatty acid synthesis, was found as a chloroplast-localized protein (Figure 2H and Supplementary information, Figure S1). The distinctive subcellular localization patterns of *SOM3* and *MOD1* suggest that the cell death modulated by these two proteins involves an active information exchange between chloroplasts and mitochondria. *SOM3* is a subunit of complex I, and disruption of *AT1G47260* (*SOM3*) reduces complex I levels [15]. We also found that the mutation of *SOM3* protein, which is undetectable in the *som3* mutants (Figure 2I), perturbed the NADH oxidase activities (Figure 2J) of complex I. These results suggested that an intact complex I is possibly required for the *MOD1*-mediated PCD.

som42 modulates complex I through specifically regulating *NAD7*

Among other *mod1* suppressors, we also identified a

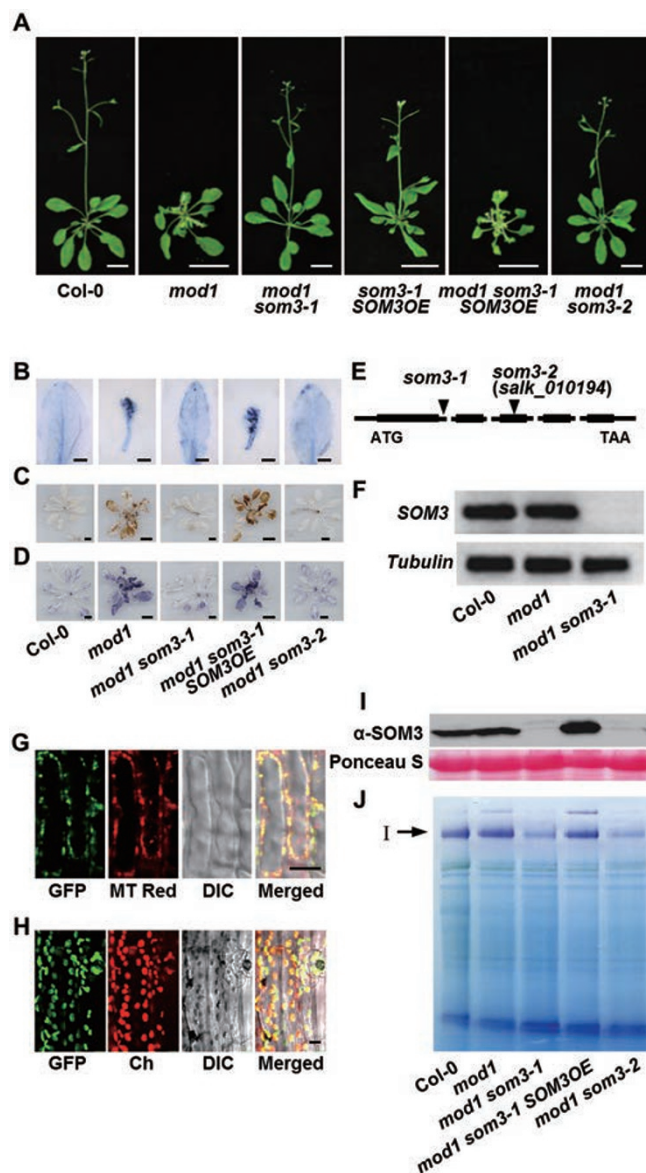


Figure 2 Characterization and cloning of *som3*. (A) Phenotypes of Col-0, *mod1*, *mod1 som3-1*, *som3-1 SOM3OE* (*SOM3* overexpression driven by the 35S promoter in the *mod1 som3-1* background), *mod1 som3-1 SOM3OE*, and *mod1 som3-2* (*SALK_010194 mod1*). Scale bar, 2 cm. (B) Leaves stained with Trypan blue, showing their cell death phenotype. Scale bar, 0.2 cm. (C, D) Seedlings stained with DAB (C) and NBT (D), respectively. Scale bar, 1 cm. (E) Physical map of the T-DNA insertion sites in the gene *AT1G47260*. (F) RT-PCR showing the expression levels of *SOM3*. (G, H) Subcellular localization of *SOM3-GFP* (G) and *MOD1-GFP* (H) in stable transgenic plants. The fluorescence of *SOM3* merged with the fluorescence of mitochondrial-specific dye MT Red (MitoTracker Red). Ch, chloroplast. Scale bar, 10 μ m. (I) Western blot showing *SOM3* protein contents. (J) In-gel assay of NADH oxidase activity. The activity staining bands on the lower part of the gel corresponds to the activity of the dehydrolipoamide dehydrogenase, which can act as a loading control. I, mitochondrial complex I.

dominant one, *mod1 som42*, which can partially suppress the *mod1* phenotypes (Figure 3A-3D). Molecular characterization of *som42* showed that the suppression might result from a T-DNA insertion in the promoter region of *AT2g01390* (Figure 3E). Reverse transcription-quantitative-PCR (RT-qPCR) analysis revealed that the expression level of *AT2g01390* was significantly increased in *mod1 som42* compared with the wild-type plants (Figure 3F), consistent with the gain-of-function mutation nature of *som42*. Furthermore, overexpression of the

AT2g01390 gene showed that the *mod1* mutant phenotypes, including plant development, cell death and ROS accumulation, could be completely suppressed (Figure 3A-3D and 3F). Therefore, *AT2g01390* is the *SOM42* gene, and its overexpression is responsible for the suppression of the *mod1* phenotypes.

SOM42 is a nuclear-encoded PPR protein, which belongs to the P subfamily of the PPR family (Supplementary information, Figure S2A) with highly conserved homologous proteins in higher plants (Supplementary in-

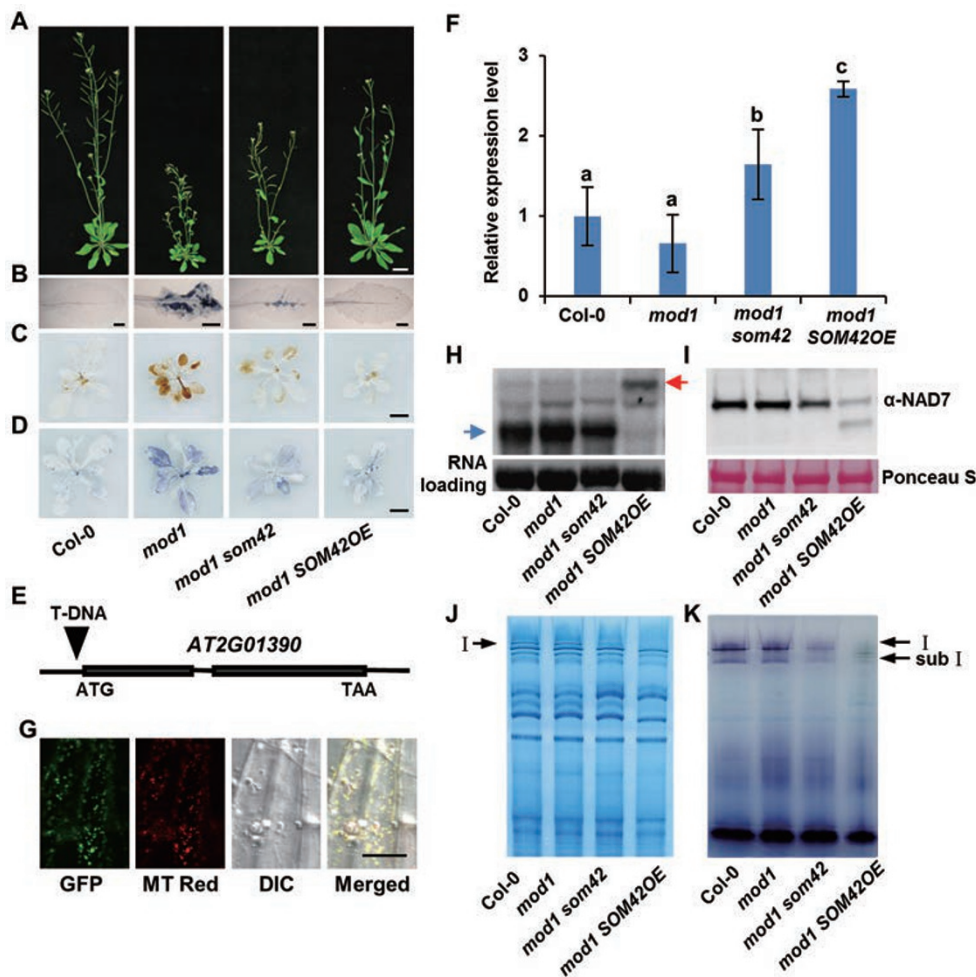


Figure 3 Characterization and cloning of *som42*. **(A)** Phenotypes of Col-0, *mod1*, *mod1 som42*, and *mod1 SOM42OE* (*SOM42* overexpression driven by the 35S promoter in the *mod1* background). Scale bar, 2 cm. **(B)** Leaves stained with Trypan blue. Scale bar, 0.2 cm. **(C, D)** Seedlings stained with DAB **(C)** and NBT **(D)**, respectively. Scale bar, 1 cm. **(E)** Physical map of the T-DNA insertion site. The T-DNA is inserted in the promoter region of *AT2G01390*, 183 bp upstream of the ATG start codon. **(F)** The expression levels of *SOM42* revealed by RT-qPCR using β -*tubulin* as reference. Values are means \pm SD of three technical replicates, and similar results were obtained in three independent experiments. Statistical differences are indicated with lowercase letters ($P < 0.05$, one-way ANOVA). **(G)** Subcellular localization of *SOM42*-GFP in 35S:*SOM42*-GFP transgenic plants. MT Red, MitoTracker Red. Scale bar, 20 μ m. **(H)** Northern blot showing the transcription levels of *NAD7* probed with exon 3. The blue arrow refers to the mature transcripts of *NAD7* and the red arrow refers to the immature transcripts of *NAD7*. **(I)** Western blot showing the protein contents of *NAD7*. **(J)** Complex I protein stained with Coomassie blue. I, mitochondrial complex I. **(K)** In-gel assay of NADH oxidase activity. I, mitochondrial complex I; sub I, mitochondrial sub-complex I.

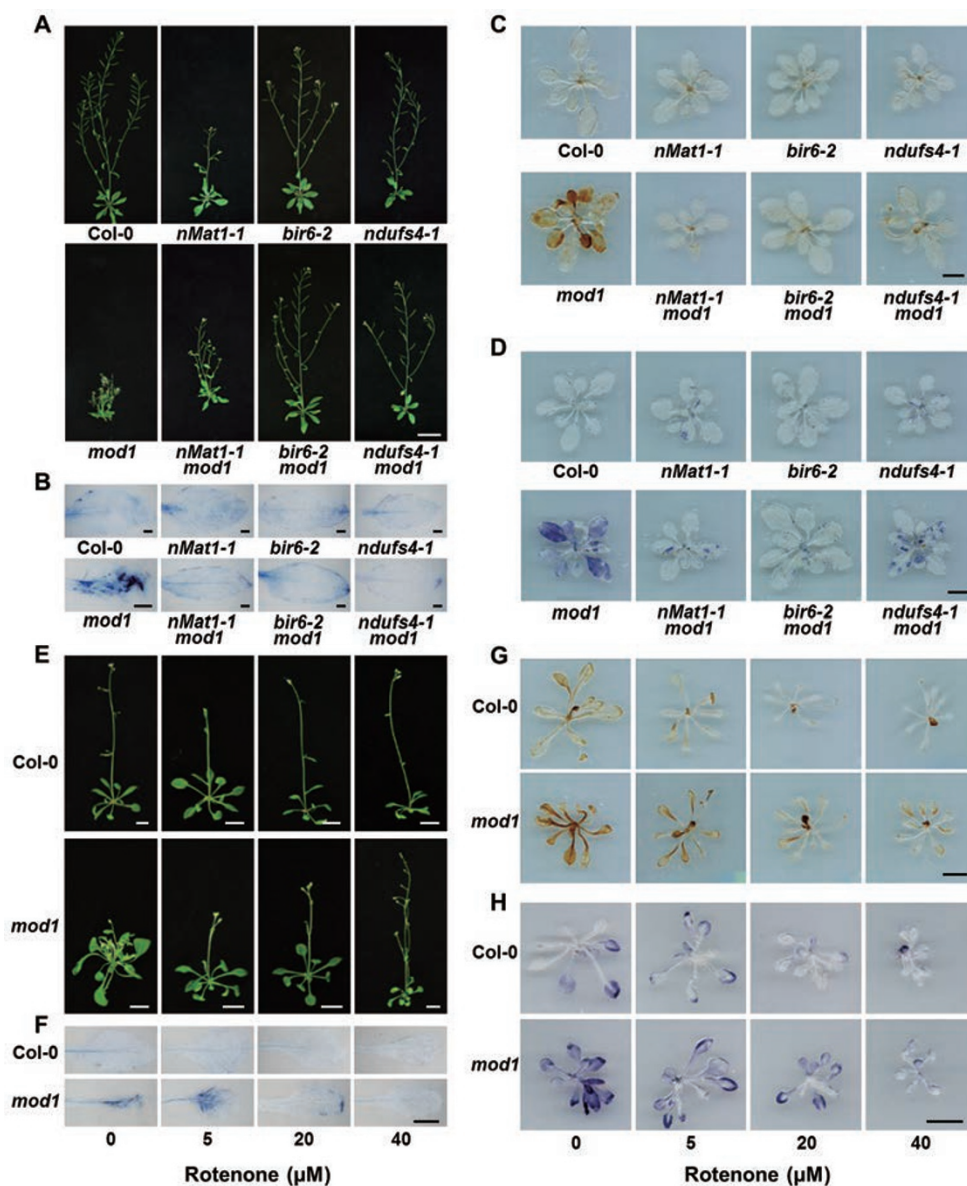


Figure 4 Suppression of *mod1* cell death by mitochondrial complex I-deficient mutants and rotenone treatment. **(A)** Phenotypes of *mod1*, mitochondrial complex I-deficient mutants and their double mutants. Scale bar, 4 cm. **(B)** Leaves stained with Trypan blue. Scale bar, 0.2 cm. **(C)** DAB-stained seedlings. Scale bar, 1 cm. **(D)** NBT-stained seedlings. Scale bar, 1 cm. **(E)** Phenotypes of Col-0 and *mod1* mutant plants following rotenone treatment. Scale bar, 1 cm. **(F)** Trypan blue-stained leaves of plants following rotenone treatment. Scale bar, 0.2 cm. **(G)** DAB-stained seedlings following rotenone treatment. Scale bar, 1 cm. **(H)** NBT-stained seedlings following rotenone treatment. Scale bar, 1 cm.

formation, Figure S2B), some of which have been localized in plastids or mitochondria [18, 27, 34]. As shown in Figure 3G, SOM42, similar to SOM3, was also localized in the mitochondria. In mitochondria, PPR proteins have been found to affect the maturation of complex I *NAD* transcripts, which are transcribed from the mitochondrial genomes [14, 35, 36]. RT-qPCR analysis showed that *NAD7* transcripts were remarkably decreased in both

mod1 som42 and *SOM42*-overexpressing lines (Supplementary information, Figure S3), indicating that SOM42 is specifically involved in the maturation of the *NAD7* transcripts, which was further confirmed by northern blot analysis (Figure 3H). Consequently, the accumulation of *NAD7* protein was substantially reduced (Figure 3I). It has been reported that the decrease in the *NAD7* protein level could impair the abundance and function of com-

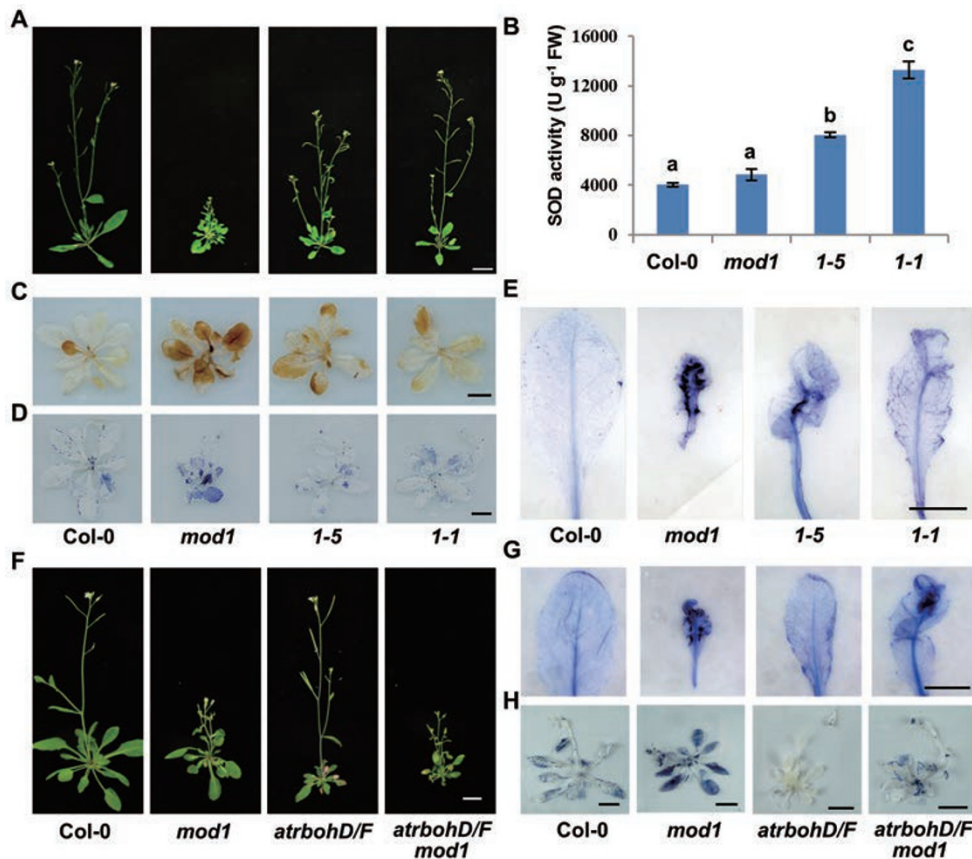


Figure 5 Effects of *CSD1* overexpression and knockout of NADPH oxidase genes in the *mod1* background. **(A)** Phenotypes of Col-0, *mod1* and 35S:*CSD1/mod1* transgenic plants (1-1 and 1-5 independent lines). Scale bar, 1 cm. **(B)** SOD activities of Col-0, *mod1* and 35S:*CSD1/mod1* transgenic plants. Statistical differences are indicated with lowercase letters ($P < 0.01$, one-way ANOVA). Similar results were obtained in three independent experiments. **(C)** DAB-stained seedlings. Scale bar, 1 cm. **(D)** NBT-stained seedlings. Scale bar, 1 cm. **(E)** Leaves stained with Trypan blue. Scale bar, 0.5 cm. **(F)** Phenotypes of Col-0, *mod1*, *atrbohD atrbohF* (*atrbohD/F*) and *atrbohD/F mod1*. Scale bar, 1 cm. **(G)** Leaves stained with Trypan blue. Scale bar, 0.5 cm. **(H)** NBT-stained seedlings. Scale bar, 2 cm. See also Supplementary information, Figure S7.

plex I [18, 21]. We therefore analyzed the protein level and NADH oxidase activities of complex I, and found that both were apparently reduced in *mod1 som42* and severely decreased in *SOM42*-overexpressing transgenic plants compared with the wild type (Figure 3J and 3K). Taken together, these results demonstrated that *SOM42* negatively regulates complex I activity by modulating the *NAD7* transcripts, which encodes a key component of complex I.

Deficiency in complex I suppresses the *mod1* phenotypes

To investigate whether the specific reduction of complex I activity is sufficient to suppress the *mod1* phenotypes, we first analyzed the effects of the mutations in key components or regulatory factors of complex I, including *nMAT1*, *BIR6* and *NDUFS4*. The *nMAT1* protein is a nuclear maturase that affects *NAD1*, *NAD2* and

NAD4 splicing [17, 37], and *BIR6* is a PPR protein that affects the splicing of *NAD7* intron 1 [18]. *NDUFS4* is a nuclear-encoded subunit of complex I [20]. Mutations in these genes cause defects in complex I. We crossed *mod1* with *nMat1-1* (CS808228), *bir6-2* (SALK_000310) and *ndufs4-1* (CS825412), respectively, and analyzed the phenotypes of the resulting double mutants. We found that all these double mutations were able to suppress the growth defects (Figure 4A), cell death (Figure 4B) and accumulation of ROS (Figure 4C and 4D) in *mod1*, which was correlated with the reduction in the NADH oxidase activities of complex I (Supplementary information, Figure S4). It should be pointed out that although the ROS levels of the double mutants between *mod1* and individual mitochondrial complex I-deficient mutants including *ndufs4-1* were much lower than that of *mod1*, they were still higher than that of the wild type (Figure

4D and Supplementary information, Figure S5), which is consistent with previous reports [16, 20, 38]. Therefore, it is the mutations in complex I components that cause the suppression of the *mod1* phenotypes.

To reinforce the genetic analysis data, we treated *mod1* seedlings with rotenone, a specific inhibitor of complex I, which blocks the transfer of electrons from the iron-sulfur centers in complex I to ubiquinone [39]. Treatment with rotenone partially rescued the *mod1* phenotypes exemplified by alleviated cell death (Figure 4E, 4F and Supplementary information, Figure S6A) and reduced accumulation of H₂O₂ and O₂⁻ in *mod1* (Figure 4G, 4H and Supplementary information, Figure S6B), which are similar to those observed in *mod1* and complex I double mutants. Taken together, these genetic and physiological studies demonstrated that the *mod1*-modulated ROS generation and cell death essentially depend on a functional complex I.

Overexpression of SOD rescues *mod1* phenotypes

Data presented above indicate that *mod1*-triggered cell death requires a functional complex I, which may be caused by ROS generated from electron transfer. To test this possibility, we attempted to reduce ROS via overexpressing the *Arabidopsis* cytosolic Cu/Zn SOD (*CSD1*) [40] in *mod1*. We found that the *mod1* mutant phenotypes were mostly rescued in *CSD1*-overexpressing transgenic plants (Figure 5A), and the degree of the rescue *mod1* phenotypes was well correlated with SOD enzymatic activities (Figure 5B), ROS reduction (Figure 5C and 5D) and attenuation of cell death (Figure 5E). Collectively, these results demonstrated that ROS generated from mitochondrial ETC plays an important role in regulating *mod1*-triggered cell death.

ROS generated by NADPH oxidase is not responsible for mod1 cell death

The *Arabidopsis* respiratory burst oxidase homolog (*AtRBOH*) family genes, *AtRBOHD* and *AtRBOHF*, have been shown to play a role in the plant defense re-

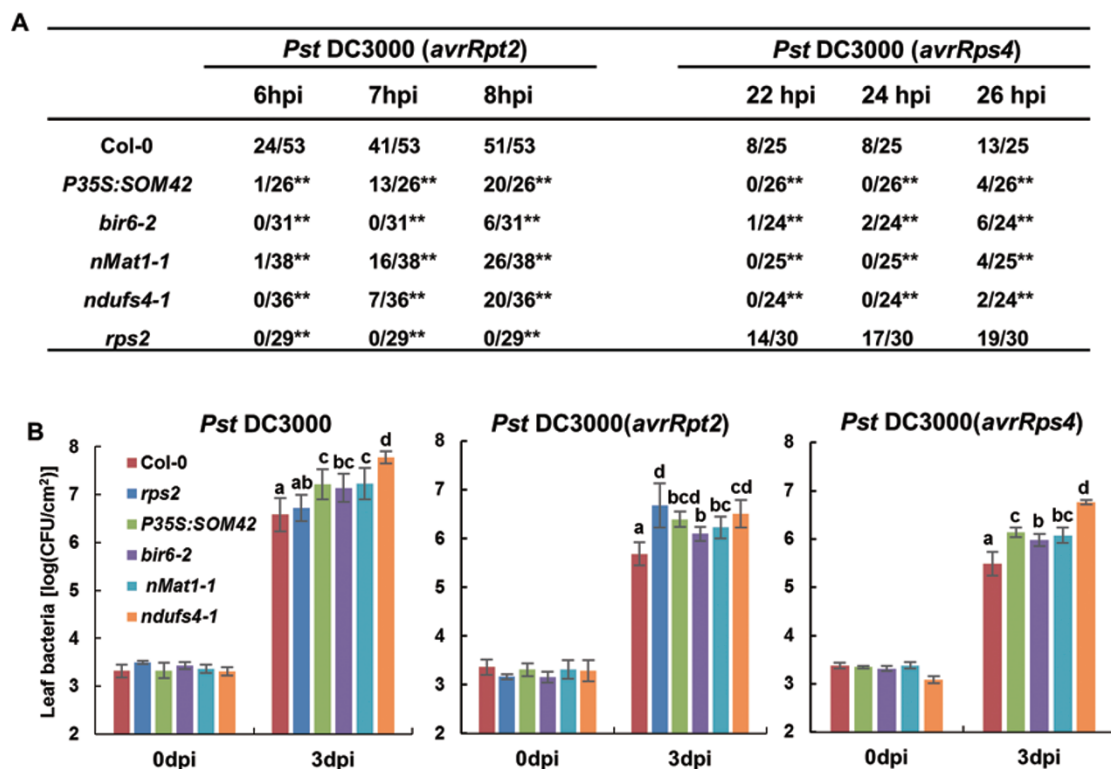


Figure 6 Bacterial defense analyses. **(A)** Deficiency in complex I inhibits both the RPS2- and RPS4-dependent HR. The ratio shows the HR leaves to the total number of leaves injected. hpi, hours postinfection. Significant differences compared with Col-0 are indicated by asterisks for $P < 0.01$ (**) using the binomial test (one-tailed). **(B)** Analysis of bacterial growth 3 days after infiltration of 10^6 cfu/ml of *Pst* DC3000 expressing empty vector, *avrRpt2* or *avrRps4* into the indicated plants. Eight plants were used for each genotype. The bars represent means \pm SD. Statistical differences are indicated with lowercase letters ($n = 8$, $P < 0.01$, one-way ANOVA). The experiment was repeated more than two times with similar results. CFU, colony-forming units; dpi, day(s) postinfection.

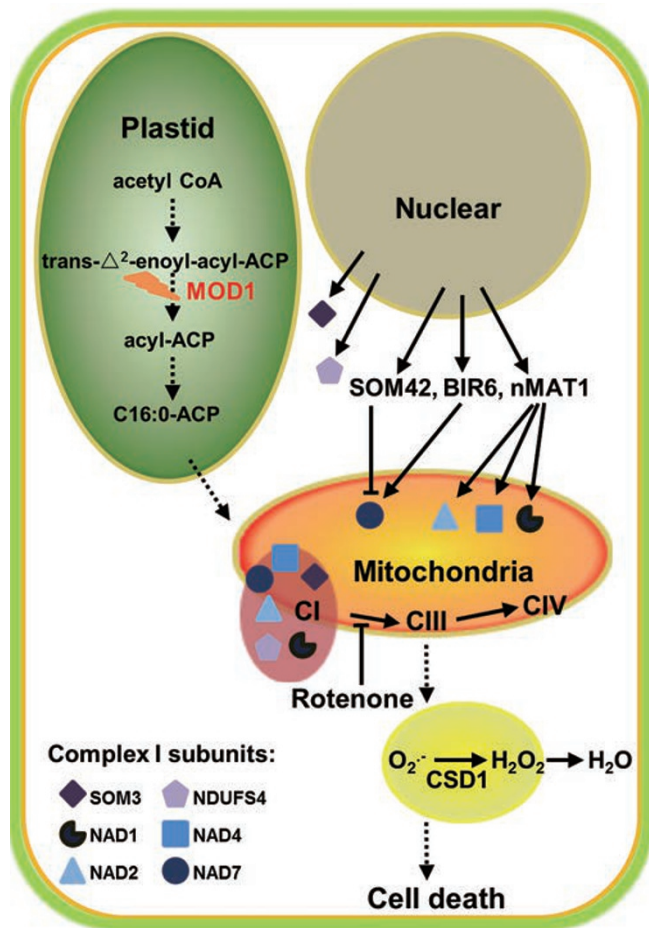


Figure 7 A proposed model of programmed cell death in *mod1*. A proposed signalling pathway, showing the initiation and suppression of the *mod1* cell death. A deficiency in the fatty acid biosynthesis in chloroplasts leads to the generation of an unidentified signal, which induces the formation of ROS through the mitochondrial ETC to initiate the PCD process in *mod1* plants. Mutations (*som3*, *som42*, *bir6-2*, *nMat1-1*, and *ndufs4-1*) or chemicals that affect the electron transfer along the ETC to form ROS can suppress the phenotypes of *mod1* mutant plants, suggesting that the ROS generated in mitochondria through ETC, plays an essential role in triggering plant PCD. SOM3 and NDUFS4 are nuclear-encoded subunits of complex I, while NAD1, NAD2, NAD4, and NAD7 are mitochondria-encoded subunits of complex I. The nMAT1 protein is a nuclear maturase that affects NAD1, NAD2 and NAD4 splicing. SOM42 and BIR6 are PPR proteins that affect the splicing of NAD7. CSD, *Arabidopsis* cytosolic Cu/Zn SOD.

sponse and HR [41, 42]. AtRBOHD and AtRBOHF are components of the plasma membrane-localized NADPH oxidase that is a main source of ROS in plants [42]. To understand whether the ROS produced by NADPH oxidase plays a role in promoting cell death in *mod1*, we generated two double mutants *atrbohD mod1* and *atr-*

bohF mod1. We found that the ROS level and *mod1* phenotypes including cell death were not apparently affected (Supplementary information, Figure S7). As *AtrbohD* and *AtrbohF* are functionally redundant in ROS generation [42], we then generated a triple mutant, *atrbohD atrbohF mod1*, to compare its phenotypes with those of wild-type, *mod1* and *mod1* suppressors. As shown in Figure 5F and 5G, the morphology and cell death of the triple mutant plants were highly similar to those of the *mod1* mutant plants, although the formation of ROS by NADPH oxidase was blocked in the *atrbohD atrbohF* double mutant plants (Figure 5H). These results indicate that the ROS generated by the plasma membrane NADPH oxidase is not directly involved in the signaling pathway of *mod1* cell death.

Deficiencies in complex I compromise HR and resistance against bacteria

HR is a localized PCD in plants and is tightly associated with ROS. To explore the possible involvement of MOD1-modulated cell death in the defense responses, we examined the HR phenotype of the complex I-deficient mutants challenged by *Pseudomonas syringae* pv *tomato* DC3000 (*Pst* DC3000) carrying *avrRpt2* or *avrRps4*, which are recognized by immune receptors RPS2 or RPS4 [43-45]. We found that all these mutants, including *nMat1-1*, *bir6-2*, *ndufs4-1* and *SOM42*-overexpressing transgenic plants, showed attenuated HR induced by both *avrRpt2* and *avrRps4* (Figure 6A and Supplementary information, Figure S8), strongly suggesting that complex I plays an important role in effector-triggered HR.

We also measured the effect of complex I-deficient mutants on bacterial growth (Figure 6B). Unlike *rps2*, complex I-deficient mutants were more susceptible to *Pst* DC3000 harboring an empty vector, indicating that these mutants are compromised in basal resistance to this virulent bacterial strain. The growth of bacteria expressing *avrRpt2* or *avrRps4* was also enhanced in the complex I-deficient mutants. In addition, *ndufs4-1* resembled the fully susceptible *rps2* mutant in *Pst* DC3000(*avrRpt2*) inoculations and was more susceptible to *Pst* DC3000 and *Pst* DC3000(*avrRps4*) compared to other complex I-deficient mutants. This was consistent with the more severe deficiency of complex I activity in this mutant (Supplementary information, Figure S4). Therefore, deficiency in complex I is most likely involved in basal defense.

Discussion

As a genetically regulated process, PCD is essential for development and defenses in multicellular organisms.

Although mitochondria and mitochondria-derived ROS have been found to play a key role in triggering PCD in animals, their functions are still elusive in plant PCD. In this paper we address these critical questions by isolation and in-depth analyses of *som* mutants. As summarized in Figure 7, a deficiency in the fatty acid biosynthesis in chloroplasts results in an unidentified signal, which induces the formation of ROS through the mitochondrial ETC to initiate the PCD process in *mod1* plants. Mutations or chemicals that impair or block the transfer of electrons along the ETC to form ROS efficiently suppress the phenotypes of *mod1* mutant plants, indicating that the ROS generated in mitochondria through ETC plays an essential role in triggering plant PCD.

The identification of both *som3* and *som42* and the further characterization of their wild-type alleles as a component and a regulator of complex I, respectively, strongly suggest that the mitochondrial complex I plays a critical role in mediating PCD in plants. Mitochondria and chloroplasts are thought to originate from prokaryotes during endosymbiotic evolution in eukaryotic cells. Intimate communications among organelles are necessary to coordinate their activities during growth, development and other physiological processes [24, 46]. In this study, we clearly showed that the chloroplast-controlled cell death is mediated by mitochondria-derived ROS. It is reasonable to assume that an intracellular mobile signal is transported from chloroplasts to mitochondria to trigger PCD, which should be elucidated in the future investigation.

Many nuclear-encoded PPR proteins have been reported to regulate the gene expression of mitochondria-encoded complex I subunits in plants [14, 35, 36, 47]. Here we found that SOM42, a member of P subfamily PPR proteins, specifically affects the mitochondrial complex I subunit *NAD7* maturation (Figure 3). The results that in *SOM42*-overexpressing lines *NAD7* transcripts were significantly reduced and other *NAD* gene transcripts were dramatically increased (Supplementary information, Figure S3) support a feedback control mechanism as previously reported in *NAD3* or mETC [22, 23]. Since complex I is the first step in the respiratory redox pathway, it is not surprising that many nuclear-encoded proteins are required to regulate this highly sophisticated complex so that mitochondrial functions can be modulated to accommodate unfavorable environments. The fact that most of the *som* mutants identified in this study are complex I-deficient mutants (Supplementary information, Figure S9) suggests that *mod1* plants provide a suitable genetic tool for screening mutants defective in the subunits of complex I to dissect the function of this complicated complex.

Along the mitochondrial ETC, complex I and complex III are the main source of ROS [7]. The deficiency of complex I will certainly block electron flow into complex III and may reduce ROS generation from complex III, which is supported by treatment of *mod1* plants with rotenone, a widely used specific inhibitor of complex I that can induce the formation of ROS from complex I but inhibit the ROS formation from complex III in animals [48, 49]. This result suggests that the ROS generated from the complex III plays a major role in triggering *mod1* cell death.

In plants, plasma membrane NADPH oxidases and chloroplasts have been considered to play key roles in the execution of HR [42, 50, 51]. However, direct evidence linking mitochondrial functions to HR or disease resistance is lacking. The finding that the intact mitochondrial ETC is required for the induction of HR upon activation of RPS2 and RPS4, which belong to CC-NB-LRR and TIR-NB-LRR R proteins, respectively [52], suggests that mitochondria play an important role in HR. We also found that the resistance against both virulent and avirulent bacteria is compromised in complex I-deficient mutants. These results indicate that the mitochondria play a role in universal defense signaling. MOD1 is the target of several diphenyl ether toxins, including natural phytotoxins produced by several fungal plant pathogens [53], suggesting that saprotrophic fungi utilize the MOD1-mediated cell death pathway to aid colonization. Taken together, these data suggest that mitochondria play a pivotal role in pathogen resistance. In animals, mitochondria play a fundamental role in triggering different types of cell death involved in immunity and development [54, 55], and dysfunction of the mitochondrial ETC also causes many diseases [56, 57]. Considering that the mechanisms of cell death execution via regulating the mitochondrial complex I are conserved in different organisms, the mitochondrion-dependent cell death pathway in plants may also have important roles in regulating plant development and defense.

Materials and Methods

Plant materials and growth conditions

Seeds of *Arabidopsis thaliana* wild-type Col-0 and mutants were sterilized and planted on agar plates containing 0.5× MS with 1.0% (w/v) sucrose. Seeds were vernalized for 3–4 days at 4 °C and were placed in growth room. Seedlings (about one week old) were transferred to soil as described previously [29]. The mutants *som3-2* (SALK_010194), *nMat1-1* (CS808228), *bir6-2* (SALK_000310), *ndufs4-1* (CS825412) and *atrbohD/F* (CS9558) are T-DNA insertion lines obtained from *Arabidopsis* Biological Research Center and their genotypes were confirmed by PCR analyses. The primer sequences used for genotyping are listed in

Supplementary information, Table S1.

RNA analysis

Total RNA was prepared from 3–4-week-old seedlings using a TRIzol kit according to the user manual (Cat# 15596-026, Invitrogen) and 12.5 µg of total RNA was treated with DNase I and used for cDNA synthesis with RT kit (Cat# A3500, Promega). RT-qPCR experiments were performed using the Bio-Rad CFX96 System. The primer sequences used for RT-qPCR are listed in Supplementary information, Table S2. RNA gel-blot analysis was carried out as described previously [58]. RNA (20 µg per lane) was separated in a 0.8% (w/v) agarose gel containing 10% (v/v) formaldehyde, blotted onto a Hybond N⁺ membrane (Amersham) and probed with the PCR-amplified DNA fragments using specific primers (Supplementary information, Table S2).

Screening for suppressors

The estradiol-inducible activation vector pER16 [59] was introduced into *Agrobacterium tumefaciens* strain EHA105 by electroporation and *Arabidopsis* plants were transformed via vacuum infiltration [60]. Transformants (T₁ and T₂) were selected on plates containing 50 mg/l kanamycin and transferred to soil for phenotype observation under continuous illumination.

Cloning of gene by TAIL-PCR

The pER16-tagged genomic sequences were recovered by TAIL-PCR [61], and the PCR fragments were analyzed by DNA sequencing. Primers across the T-DNA insert were designed for genotyping, and T-DNA specific primers and arbitrary degenerate primers used for TAIL-PCR are listed in Supplementary information, Table S1.

Trypan blue staining

Trypan blue staining was performed as previously described [62, 63]. Samples were covered with an alcoholic lactophenol trypan blue mixture (30 ml ethanol, 10 g phenol, 10 ml water, 10 ml glycerol, 10 ml lactic acid and 10 mg trypan blue), placed in a boiling water bath for 2–3 min, and then left at room temperature for 1 h. The samples were transferred into a chloral hydrate solution (2.5 g/ml) and boiled for 20 min to destain. After multiple exchanges of chloral hydrate solution to reduce the background, samples were equilibrated with 50% (v/v) glycerol, mounted and observed with a stereomicroscope (Olympus SZX-12).

In situ detection of ROS

In situ detection of O₂⁻ and H₂O₂ were performed as described by Ramel [64] with 4–5-week-old seedlings. For *in situ* detection of O₂⁻, plantlets were immersed and infiltrated under vacuum with 1 mg/ml NBT (N6876, Sigma-Aldrich) staining solution in potassium phosphate buffer (10 mM) with 10 mM Na₂S₂O₃. After infiltration for 2–3 h, stained plantlets were boiled in acetic acid: glycerol: ethanol (1:1:3, v/v/v) solution for 10 min. Samples were then stored in 95% (v/v) ethanol until scanning. O₂⁻ was visualized as a blue color produced by NBT reduction to formazan. For *in situ* detection of H₂O₂, the staining agent, DAB (D5637, Sigma-Aldrich), was dissolved in H₂O and adjusted to pH 3.8 with HCl. The DAB solution was freshly prepared to prevent auto-oxidation. Samples were immersed and infiltrated under vacuum with 1 mg/ml DAB staining solution. Stained plantlets were then boiled in acetic

acid: glycerol: ethanol (1:1:3, v/v/v) solution for 10 min, and then stored in 95% (v/v) ethanol until scanning. H₂O₂ was visualized as a brown color due to DAB polymerization.

Plasmid construction

To construct plant transformation and transient expression plasmids, fragments containing the full-length CDS of *SOM3*, *SOM42*, *MOD1*, *CSD1* and *NAD7* were digested and ligated into respective vectors. All the genes, plasmids, primers and the cleavage sites were listed in Supplementary information, Table S3.

Subcellular localization

To obtain transformed *Arabidopsis* lines, T₂ transgenic plants showing a restored phenotype were genetically analyzed and homozygous transgenic lines were selected for in-depth analysis. Staining of mitochondrial-specific dye was performed as described previously [65], and the GFP signal and fluorescence of MitoTracker Red were examined under a confocal microscope at an excitation wavelength of 488 nm and 543 nm, respectively (FluoView 1000, Olympus). To carry out the transient expression analysis of MOD1-GFP, *Arabidopsis* mesophyll protoplasts were isolated and transformed as described previously [66], and GFP signals were detected by a confocal fluorescence microscope (FluoView 1000, Olympus).

Assays of enzyme activities of complex I and SOD

Analyses of the NADH oxidase activity and the protein abundance of the mitochondrial complex I were performed as described previously [19]. Proteins of crude membrane extract from 3–4-week-old seedlings were solubilized with 1% (v/v) digitonin and resolved by Blue Native-PAGE. To measure the SOD activity, seedlings were homogenized in liquid nitrogen, then 1 ml extraction buffer consisting of 50 mM sodium phosphate (pH 7.8) and 1% (w/v) polyvinylpyrrolidone was added to 0.1 g material sample. After centrifugation at 10 000 rpm for 5 min at 4 °C, the supernatant containing SOD was used for measuring the SOD activity with the SOD Assay Kit-WST according to the user's directions (Dojindo).

Inhibitor treatment

The respiration inhibitor rotenone (Sigma-Aldrich) was dissolved in Dimethyl sulfoxide at concentration of 0.25 M, and then added to MS media at a final concentration of 5, 20 and 40 µM, respectively, and plates or tissue culture bottles were placed in an incubator under continuous illumination at 26 °C.

Preparation of polyclonal antibodies

The CDS of *SOM3* or *NAD7* was amplified with the primer pair (Supplementary information, Table S3) and subcloned into pE-T28a. Recombinant *SOM3* and *NAD7* proteins were expressed in BL21 cells and applied to raise polyclonal antibodies in rabbit and mouse, respectively.

Protein extraction and western blot analysis

Arabidopsis seedlings or leaves were grounded into powders in liquid nitrogen and total proteins were extracted using the extraction buffer (500 mM Tris-HCl, pH 7.5, 150 mM NaCl, 0.1% NP-40, 4 M urea, 1 mM phenylmethanesulfonyl fluoride). After the centrifugation at 13 000 rpm for 10 min at 4 °C, the supernatant was

transferred into a new tube and quantified by the Bio-Rad protein assay. Protein blots were performed with the SuperSignal West chemiluminescence kit according to the manufacturer's protocol (Pierce Chemical).

Bacterial growth and HR assays

Bacterial growth and HR assays were performed as previously described [67]. Briefly, for bacterial growth assay, 5-week-old *Arabidopsis* leaves under a 10/14 h light/dark photoperiod at 23 °C were infiltrated with *Pst* DC3000 bacteria at 10⁶ CFU/ml. The bacterial growth in the leaves was counted at the indicated times. For the HR assay, plants were infiltrated with 10⁸ CFU/ml *Pst* DC3000 (*avrRpt2*) or *Pst* DC3000(*avrRps4*).

Additional methods are described in the Supplementary information, Data S1.

Acknowledgments

We thank Xinnian Dong (Duke University) for critically reading the manuscript and Weicai Yang (Institute of Genetics and Developmental Biology, Chinese Academy of Sciences) for providing the pWM101 vector. This work was supported by grants from the National Natural Science Foundation of China (30830009, 91335204) and the Chinese Academy of Sciences.

References

- Lam E. Controlled cell death, plant survival and development. *Nat Rev Mol Cell Biol* 2004; **5**:305-315.
- Wang C, Youle RJ. The role of mitochondria in apoptosis. *Annu Rev Genet* 2009; **43**:95-118.
- Marchi S, Giorgi C, Suski JM, et al. Mitochondria-ros cross-talk in the control of cell death and aging. *J Signal Transduct* 2012; **2012**:329-635.
- Suzuki N, Miller G, Morales J, Shulaev V, Torres MA, Mittler R. Respiratory burst oxidases: the engines of ROS signaling. *Curr Opin Plant Biol* 2011; **14**:691-699.
- Zurbriggen MD, Carrillo N, Hajirezaei MR. ROS signaling in the hypersensitive response: when, where and what for? *Plant Signal Behav* 2010; **5**:393-396.
- Coll NS, Epple P, Dangl JL. Programmed cell death in the plant immune system. *Cell Death Differ* 2011; **18**:1247-1256.
- Andreyev AY, Kushnareva YE, Starkov AA. Mitochondrial metabolism of reactive oxygen species. *Biochemistry* 2005; **70**:200-214.
- Apel K, Hirt H. Reactive oxygen species: metabolism, oxidative stress, and signal transduction. *Annu Rev Plant Biol* 2004; **55**:373-399.
- Fearnley IM, Carroll J, Walker JE. Proteomic analysis of the subunit composition of complex I (NADH:ubiquinone oxidoreductase) from bovine heart mitochondria. *Methods Mol Biol* 2007; **357**:103-125.
- Carroll J, Fearnley IM, Shannon RJ, Hirst J, Walker JE. Analysis of the subunit composition of complex I from bovine heart mitochondria. *Mol Cell Proteomics* 2003; **2**:117-126.
- Klodmann J, Sunderhaus S, Nimtz M, Jansch L, Braun HP. Internal architecture of mitochondrial complex I from *Arabidopsis thaliana*. *Plant Cell* 2010; **22**:797-810.
- Adams KL, Palmer JD. Evolution of mitochondrial gene content: gene loss and transfer to the nucleus. *Mol Phylogeny Evol* 2003; **29**:380-395.
- Brandt U. Energy converting NADH:quinone oxidoreductase (complex I). *Annu Rev Biochem* 2006; **75**:69-92.
- Juszczuk IM, Szal B, Rychter AM. Oxidation-reduction and reactive oxygen species homeostasis in mutant plants with respiratory chain complex I dysfunction. *Plant Cell Environ* 2012; **35**:296-307.
- Perales M, Eubel H, Heinemeyer J, Colaneri A, Zabaleta E, Braun HP. Disruption of a nuclear gene encoding a mitochondrial gamma carbonic anhydrase reduces complex I and supercomplex I + III₂ levels and alters mitochondrial physiology in *Arabidopsis*. *J Mol Biol* 2005; **350**:263-277.
- Lee BH, Lee H, Xiong L, Zhu JK. A mitochondrial complex I defect impairs cold-regulated nuclear gene expression. *Plant Cell* 2002; **14**:1235-1251.
- Nakagawa N, Sakurai N. A mutation in *At-nMat1a*, which encodes a nuclear gene having high similarity to group II intron maturase, causes impaired splicing of mitochondrial *NAD4* transcript and altered carbon metabolism in *Arabidopsis thaliana*. *Plant Cell Physiol* 2006; **47**:772-783.
- Koprivova A, des Francs-Small CC, Calder G, et al. Identification of a pentatricopeptide repeat protein implicated in splicing of intron 1 of mitochondrial *nad7* transcripts. *J Biol Chem* 2010; **285**:32192-32199.
- Pineau B, Layoune O, Danon A, De Paepe R. L-galactono-1,4-lactone dehydrogenase is required for the accumulation of plant respiratory complex I. *J Biol Chem* 2008; **283**:32500-32505.
- Meyer EH, Tomaz T, Carroll AJ, et al. Remodeled respiration in *ndufs4* with low phosphorylation efficiency suppresses *Arabidopsis* germination and growth and alters control of metabolism at night. *Plant Physiol* 2009; **151**:603-619.
- Dutilleul C, Garmier M, Noctor G, et al. Leaf mitochondria modulate whole cell redox homeostasis, set antioxidant capacity, and determine stress resistance through altered signaling and diurnal regulation. *Plant Cell* 2003; **15**:1212-1226.
- Zhu Q, Dugardeyn J, Zhang C, et al. The *Arabidopsis thaliana* RNA editing factor SLO2, which affects the mitochondrial electron transport chain, participates in multiple stresses and hormone responses. *Mol Plant* 2014; **7**:290-310.
- Yuan H, Liu D. Functional disruption of the pentatricopeptide protein SLG1 affects mitochondrial RNA editing, plant development, and responses to abiotic stresses in *Arabidopsis*. *Plant J* 2012; **70**:432-444.
- Woodson JD, Chory J. Coordination of gene expression between organellar and nuclear genomes. *Nat Rev Genet* 2008; **9**:383-395.
- Small ID, Peeters N. The PPR motif - a TPR-related motif prevalent in plant organellar proteins. *Trends Biochem Sci* 2000; **25**:46-47.
- Schmitz-Linneweber C, Small I. Pentatricopeptide repeat proteins: a socket set for organelle gene expression. *Trends Plant Sci* 2008; **13**:663-670.
- Lurin C, Andres C, Aubourg S, et al. Genome-wide analysis of *Arabidopsis* pentatricopeptide repeat proteins reveals their essential role in organelle biogenesis. *Plant Cell* 2004; **16**:2089-2103.

- 28 O'Toole N, Hattori M, Andres C, *et al.* On the expansion of the pentatricopeptide repeat gene family in plants. *Mol Biol Evol* 2008; **25**:1120-1128.
- 29 Mou Z, He Y, Dai Y, Liu X, Li J. Deficiency in fatty acid synthase leads to premature cell death and dramatic alterations in plant morphology. *Plant Cell* 2000; **12**:405-418.
- 30 Bestwick CS, Brown IR, Bennett MH, Mansfield JW. Localization of hydrogen peroxide accumulation during the hypersensitive reaction of lettuce cells to *Pseudomonas syringae* pv *phaseolicola*. *Plant Cell* 1997; **9**:209-221.
- 31 Liu Y, Ren D, Pike S, Pallardy S, Gassmann W, Zhang S. Chloroplast-generated reactive oxygen species are involved in hypersensitive response-like cell death mediated by a mitogen-activated protein kinase cascade. *Plant J* 2007; **51**:941-954.
- 32 Parisi G, Perales M, Fornasari MS, *et al.* Gamma carbonic anhydrases in plant mitochondria. *Plant Mol Biol* 2004; **55**:193-207.
- 33 Meyer EH, Taylor NL, Millar AH. Resolving and identifying protein components of plant mitochondrial respiratory complexes using three dimensions of gel electrophoresis. *J Proteome Res* 2008; **7**:786-794.
- 34 Barkan A, Rojas M, Fujii S, *et al.* A combinatorial amino acid code for RNA recognition by pentatricopeptide repeat proteins. *PLoS Genet* 2012; **8**:e1002910.
- 35 Ichinose M, Sugita C, Yagi Y, Nakamura T, Sugita M. Two DYW subclass PPR proteins are involved in RNA editing of *ccmF* and *atp9* transcripts in the moss *Physcomitrella patens*: first complete set of PPR editing factors in plant mitochondria. *Plant Cell Physiol* 2013; **54**:1907-1916.
- 36 Hartel B, Zehrmann A, Verbitskiy D, Takenaka M. The longest mitochondrial RNA editing PPR protein MEF12 in *Arabidopsis thaliana* requires the full-length E domain. *RNA Biol* 2013; **10**:1543-1548.
- 37 Keren I, Tal L, des Francs-Small CC, *et al.* nMAT1, a nuclear-encoded maturase involved in the trans-splicing of *nad1* intron 1, is essential for mitochondrial complex I assembly and function. *Plant J* 2012; **71**:413-426.
- 38 He J, Duan Y, Hua D, *et al.* DEXH box RNA helicase-mediated mitochondrial reactive oxygen species production in *Arabidopsis* mediates crosstalk between abscisic acid and auxin signaling. *Plant Cell* 2012; **24**:1815-1833.
- 39 Earley FG, Patel SD, Ragan I, Attardi G. Photolabelling of a mitochondrially encoded subunit of NADH dehydrogenase with [³H]dihydrorotenone. *FEBS Lett* 1987; **219**:108-112.
- 40 Kliebenstein DJ, Monde RA, Last RL. Superoxide dismutase in *Arabidopsis*: an eclectic enzyme family with disparate regulation and protein localization. *Plant Physiol* 1998; **118**:637-650.
- 41 Torres MA, Jones JD, Dangl JL. Pathogen-induced, NADPH oxidase-derived reactive oxygen intermediates suppress spread of cell death in *Arabidopsis thaliana*. *Nat Genet* 2005; **37**:1130-1134.
- 42 Torres MA, Dangl JL, Jones JD. *Arabidopsis gp91^{phox}* homologues *AtrbohD* and *AtrbohF* are required for accumulation of reactive oxygen intermediates in the plant defense response. *Proc Natl Acad Sci USA* 2002; **99**:517-522.
- 43 Bent AF, Kunkel BN, Dahlbeck D, *et al.* RPS2 of *Arabidopsis thaliana*: a leucine-rich repeat class of plant disease resistance genes. *Science* 1994; **265**:1856-1860.
- 44 Gassmann W, Hinsch ME, Staskawicz BJ. The *Arabidopsis* RPS4 bacterial-resistance gene is a member of the TIR-NBS-LRR family of disease-resistance genes. *Plant J* 1999; **20**:265-277.
- 45 Mindrinos M, Katagiri F, Yu GL, Ausubel FM. The *A. thaliana* disease resistance gene RPS2 encodes a protein containing a nucleotide-binding site and leucine-rich repeats. *Cell* 1994; **78**:1089-1099.
- 46 Xiao Y, Savchenko T, Baidoo EE, *et al.* Retrograde signaling by the plastidial metabolite MEcPP regulates expression of nuclear stress-response genes. *Cell* 2012; **149**:1525-1535.
- 47 Ichinose M, Tasaki E, Sugita C, Sugita M. A PPR-DYW protein is required for splicing of a group II intron of *cox1* pre-mRNA in *Physcomitrella patens*. *Plant J* 2012; **70**:271-278.
- 48 Drose S, Brandt U. The mechanism of mitochondrial superoxide production by the cytochrome *bc1* complex. *J Biol Chem* 2008; **283**:21649-21654.
- 49 Li N, Ragheb K, Lawler G, *et al.* Mitochondrial complex I inhibitor rotenone induces apoptosis through enhancing mitochondrial reactive oxygen species production. *J Biol Chem* 2003; **278**:8516-8525.
- 50 Nomura H, Komori T, Uemura S, *et al.* Chloroplast-mediated activation of plant immune signalling in *Arabidopsis*. *Nat Commun* 2012; **3**:926.
- 51 Zurbriggen MD, Carrillo N, Tognetti VB, *et al.* Chloroplast-generated reactive oxygen species play a major role in localized cell death during the non-host interaction between tobacco and *Xanthomonas campestris* pv *vesicatoria*. *Plant J* 2009; **60**:962-973.
- 52 Dangl JL, Jones JD. Plant pathogens and integrated defence responses to infection. *Nature* 2001; **411**:826-833.
- 53 Dayan FE, Ferreira D, Wang YH, Khan IA, McInroy JA, Pan Z. A pathogenic fungi diphenyl ether phytotoxin targets plant enoyl (acyl carrier protein) reductase. *Plant Physiol* 2008; **147**:1062-1071.
- 54 Green DR, Galluzzi L, Kroemer G. Mitochondria and the autophagy-inflammation-cell death axis in organismal aging. *Science* 2011; **333**:1109-1112.
- 55 Fuchs Y, Steller H. Programmed cell death in animal development and disease. *Cell* 2011; **147**:742-758.
- 56 Taylor RW, Turnbull DM. Mitochondrial DNA mutations in human disease. *Nat Rev Genet* 2005; **6**:389-402.
- 57 Hu Y, Lu W, Chen G, *et al.* K-ras(G12V) transformation leads to mitochondrial dysfunction and a metabolic switch from oxidative phosphorylation to glycolysis. *Cell Res* 2012; **22**:399-412.
- 58 Sun F, Zhang W, Xiong G, *et al.* Identification and functional analysis of the MOC1 interacting protein 1. *J Genet Genomics* 2010; **37**:69-77.
- 59 Zuo J, Niu QW, Frugis G, Chua NH. The WUSCHEL gene promotes vegetative-to-embryonic transition in *Arabidopsis*. *Plant J* 2002; **30**:349-359.
- 60 Dai Y, Wang H, Li B, *et al.* Increased expression of MAP KINASE KINASE7 causes deficiency in polar auxin transport and leads to plant architectural abnormality in *Arabidopsis*. *Plant Cell* 2006; **18**:308-320.
- 61 Liu YG, Mitsukawa N, Oosumi T, Whittier RF. Efficient

- isolation and mapping of *Arabidopsis thaliana* T-DNA insert junctions by thermal asymmetric interlaced PCR. *Plant J* 1995; **8**:457-463.
- 62 Stone JM, Heard JE, Asai T, Ausubel FM. Simulation of fungal-mediated cell death by fumonisin B1 and selection of fumonisin B1-resistant (fbr) *Arabidopsis* mutants. *Plant Cell* 2000; **12**:1811-1822.
- 63 Bowling SA, Clarke JD, Liu Y, Klessig DF, Dong X. The *cpr5* mutant of *Arabidopsis* expresses both NPR1-dependent and NPR1-independent resistance. *Plant Cell* 1997; **9**:1573-1584.
- 64 Ramel F, Sulmon C, Gouesbet G, Couée I. Natural variation reveals relationships between pre-stress carbohydrate nutritional status and subsequent responses to xenobiotic and oxidative stress in *Arabidopsis thaliana*. *Ann Bot* 2009; **104**:1323-1337.
- 65 Hedtke B, Meixner M, Gillandt S, Richter E, Borner T, Weihe A. Green fluorescent protein as a marker to investigate targeting of organellar RNA polymerases of higher plants *in vivo*. *Plant J* 1999; **17**:557-561.
- 66 Yoo SD, Cho YH, Sheen J. *Arabidopsis* mesophyll protoplasts: a versatile cell system for transient gene expression analysis. *Nat Protoc* 2007; **2**:1565-1572.
- 67 Yao J, Withers J, He SY. *Pseudomonas syringae* infection assays in *Arabidopsis*. *Methods Mol Biol* 2013; **1011**:63-81.

(Supplementary information is linked to the online version of the paper on the *Cell Research* website.)



This work is licensed under the Creative Commons Attribution-NonCommercial-No Derivative Works 3.0 Unported License. To view a copy of this license, visit <http://creativecommons.org/licenses/by-nc-nd/3.0>